Synthesis, physicochemical and biological evaluation of technetium-99m labeled lapatinib as a novel potential tumor imaging agent of Her-2 positive breast cancer

ARTICLE *in* EUROPEAN JOURNAL OF MEDICINAL CHEMISTRY · NOVEMBER 2014

Impact Factor: 3.45 · DOI: 10.1016/j.ejmech.2014.09.080

European Journal of Medicinal Chemistry 87 (2014) 493–499

Contents lists available at ScienceDirect

European Journal of Medicinal Chemistry

journal homepage: http://www.elsevier.com/locate/ejmech

Original article

Synthesis, physicochemical and biological evaluation of technetium-99m labeled lapatinib as a novel potential tumor imaging agent of Her-2 positive breast cancer

Ewa Gniazdowska [a, *], Przemysław Koźmiński [a], Krzysztof Bańkowski [b], Wojciech Łuniewski [b], Leszek Królicki [c]

[a] Centre for Radiochemistry and Nuclear Chemistry, Institute of Nuclear Chemistry and Technology, 16 Dorodna Street, 03-195 Warsaw, Poland
[b] Pharmaceutical Research Institute, 8 Rydygiera Street, 01-793 Warsaw, Poland
[c] Nuclear Medicine Department, Medical University of Warsaw, 1a Banacha Street, 02-097 Warsaw, Poland

ARTICLE INFO

Article history:
Received 11 June 2014
Received in revised form
22 September 2014
Accepted 24 September 2014
Available online 28 September 2014

Keywords:
Lapatinib
Her-2 receptor
Technetium
Radiopharmaceutical
SKOV-3

ABSTRACT

Tumors that are Her-2-positive tend to grow and spread more quickly than other types of breast cancer. Overexpression of Her-2 can be a predictive biomarker for stratification of patients for therapy with Herceptin (containing humanized IgG1 monoclonal antibody trastuzumab) or Tykerb (containing lapatinib di-*p*-toluenesulfonate) drug. Usually, Her-2 status is determined by immunohistochemical (IHC) as well as fluorescent or chromogenic in situ hybridisation (FISH or CISH) analysis of biopsy material. The objective of the present work was to standardize the conjugation of anti-cancer drug lapatinib (which recognizes selectively the Her-2 extracellular domain) with technetium-99m complex, of type '4+1', to obtain ^{99m}Tc(NS$_3$)(CN-lapatinib) conjugate for use as *in vivo* tracer of the Her-2 expression in breast cancer. The conjugate ^{99m}Tc(NS$_3$)(CN-lapatinib) was formed with high yield, high radiochemical purity and specific activity within the range 25–30 GBq/μmol. The biological *in vitro* and *in vivo* studies of the conjugate showed its high affinity to Her-2 receptor (K_d = 3.5 ± 0.4 nM, K_i = 2.9 ± 0.5 nM, B_{max} = 2.4 ± 0.3 nM, approximate number of 2.4 × 10^6 binding sites per cell, IC_{50} = 41.2 ± 0.4 nM) and also pointed out to the clearance through the hepatic and renal route in comparable degree. Basing on these results one can conclude that ^{99m}Tc(NS$_3$)(CN-lapatinib) conjugate could be a promising radiopharmaceutical for *in vivo* diagnosis of the Her-2 status in breast with impact on treatment planning.

1. Introduction

Breast cancer is the 2nd leading cause of deaths in women and is the most common cancer among them. One third of women affected by breast cancer die due to this ailment [1]. Studies show that approximately more than 30% of breast cancer patients have tumors that are **H**uman **E**pidermal Growth Factor **R**eceptor 2 (Her-2) positive [2]. Her-2 overexpression is associated with increased tumor growth, increased rate of metastasis and decreased overall survival rate for the patient. Overexpression of Her-2 can be a prognostic biomarker for breast [3], ovarian [4,5], bladder [6] and lung [7] carcinomas. A normal breast cell may have 20 000 Her-2 receptors while a breast cancer cell can have as many as 1.5 million [8,9]. In breast cancer the overexpression of Her-2 is also a predictive biomarker for stratification of patients for Her-2-targeted therapies with anti-cancer drugs Herceptin or Tykerb [2]. Herceptin is a Her-2-specific drug (containing the humanized IgG1 monoclonal antibody, trastuzumab, mAb) approved for use by the U.S. Food and Drug Administration (FDA) in September 1998. Trastuzumab binds to extracellular domain region of the Her-2 receptor and inhibits its ability to dimerize with other Her-2 receptors blocking in this way the cell growth and accelerating cell apoptosis. Cells treated with trastuzumab undergo arrest during the G1 phase of the cell cycle what reduces their proliferation [10,11]. Tykerb (in Europe named also Tyverb) which contains lapatinib di-*p*-toluenesulfonate, is a second Her-2-specific drug approved for use by the FDA in 2007. Lapatinib molecule enters into

Abbreviations: Her-2, **H**uman **E**pidermal Growth Factor **R**eceptor 2; IHC, immunohistochemical; FISH, fluorescent in situ hybridisation; CISH, chromogenic in situ hybridisation; HPLC, high-performance liquid chromatography; n.c.a., no carrier added; RCP, radiochemical purity; RCY, radiochemical yield; NS$_3$, tris(2-mercaptoethyl)-amine; CN-BFCA, isocyanobutyric acid succinimidyl ester; PBS, Phosphate buffered saline; TFA, trifluoroacetic acid.

* Corresponding author.
E-mail address: e.gniazdowska@ichtj.waw.pl (E. Gniazdowska).

http://dx.doi.org/10.1016/j.ejmech.2014.09.080
0223-5234/

the cell interior, binds with intracellular parts of Her-2 and Her-1 receptors and inhibits receptors ability to accelerate cell transformation, cell growth and division [12]. Usually, Her-2 status is determined (HercepTest) by immunohistochemical (IHC), fluorescent in situ hybridisation (FISH) or chromogenic in situ hybridisation (CISH) analysis of biopsy material [13–16]. Nowadays intensive development of nuclear medicine in the field of cancer diagnosis and therapy takes place. The most important diagnostic and therapeutic radiopharmaceuticals, which selectively distribute within given tissues or organs, are formed by coordination compounds with diagnostic or therapeutic radiometal firmly attached to selected biologically active molecule. There are already several literature data concerning trastuzumab labeled with diagnostic (e.g. Tc-99m [17], In-111 [18], Zr-89 [19,20], Ga-67 [21], Cu-64 [22], I-131 [23,24]) and therapeutic (e.g. I-125 [23,24], Lu-177 [25], At-211 [26]) radionuclides. From among diagnostic radionuclides technetium-99m ($T_{1/2} = 6$ h, $E_\gamma = 140$ keV) is most commonly used for SPECT applications due to its favorable physical properties, ready availability from the ^{99}Mo-^{99m}Tc generator and relatively low cost [27]. It is expected that lapatinib labeled with technetium-99m (Fig. 1) may also serve as a diagnostic receptor radiopharmaceutical for determination of Her-2 expression in patients suffering from breast cancer of the Her-2-positive type.

The aim of this work was to synthesize conjugate containing technetium-99m complex of the '4+1' type and lapatinib as the biologically active molecule (Fig. 1(B)). The next step of the work was to determine physicochemical and biological properties of the conjugate important from the radiopharmaceutical point of view.

2. Material and methods

2.1. General

The conjugate ^{99m}Tc(NS$_3$)(CN-lapatinib) consists of ^{99m}Tc(III) cation coordinated by the tetradentate NS$_3$ tripodal chelator (tris(2-mercaptoethyl)-amine; 2,2′,2″-nitrilotriethanethiol) and a monodentate isocyanide species CN-BFCA (Bifunctional Coupling Agent, isocyanobutyric acid succinimidyl ester) previously coupled with lapatinib molecule.

NS$_3$ ligand. The tetradentate NS$_3$ ligand was prepared by reaction of tris(2-chloroethyl)amine hydrochloride with potassium thioacetate followed by reduction with $LiAlH_4$ [28].

Bifunctional CN–BFCA agent. The aliphatic linker CN-BFCA was synthesized according to the procedure described in Ref. [29].

^{1}H NMR (CD_3CN) δ (ppm): 2.41 (m, 2H, CH_2–C**H$_2$**–CH_2); 2.77 (t, 6H, CH_2–C**H$_2$**–C(O)–O and C(O)–C**H$_2$**–C**H$_2$**–C(O)); 3.54 (m, 2H, C–N–C**H$_2$**–CH_2).

Lapatinib. To the yellow suspension of 125 mg of lapatinib ditosylate (the active component of the drug Tykerb, CAS number 388082-78-8) in 10 mL of ethyl acetate 10 mL of aqueous solution of sodium carbonate (0.1 mg/mL) was added. The mixture was stirred at room temperature for 60 min during which time it changed into colorless. Then the upper organic layer was separated and washed twice with 10 mL of water at 40–50 °C. The volume of organic phase containing lapatinib in a form of free base was reduced in rotary evaporator and the product was lyophilized, yield ≈ 85%.

EA: calc. %: C 59.95; H 4.51; N 9.64; S 5.52; found %: C 60.15; H 4.38; N 9.81; S 5.63; MS: *m/z*: calc. 581.07; found 581.09 [M + H$^+$].

^{1}H NMR: (CD_3CN) δ (ppm): 3.04 (s, 3H, C**H$_3$**–S); 3.55 (m, 2H, CH_2–C**H$_2$**–N); 3.65 (m, 2H, S–C**H$_2$**–CH_2); 5.26 (s, 2H, O–C**H$_2$**–C); 6.90 and 7.21 (respectively, d, 1H, C–CH–CH–C and d, 1H, C–CH–CH–C, in aromatic ring of furan), 7.15, 7.29, 7.33 and 7.47 (respectively, ddd, 1H, C(F)–CH–CH–CH C, d, 1H, C–CH–C(F), m, 1H, C(F)–CH–CH–CH–C and m, 1H, C(F)–CH–CH–CH–C, in aromatic ring of fluorobenzene), 7.20, 7.44 and 7.69 (respectively, d, 1H, C(Cl)–C–CH–CH, dd, 1H, C–CH–CH–C and d, 1H, C(N)–CH–C(Cl) in aromatic ring of chlorobenzene), 8.93, 8.23 and 8.15 (respectively, s, 1H, C–CH–C, dd, 1H, C–CH–CH and d, 1H, CH–CH–C, in aromatic ring of benzene), 8.68 (s, 1H, N–C**H**–N); 8.91 (s, 2H, NH–C**H$_2$**–C); 10.99 (s, 1H, C–N**H**–C).

2.2. Synthesis of CN-lapatinib

The coupling reaction of the isocyanide linker CN-BFCA with the lapatinib molecule (Scheme 1) was performed according to the procedure described in Ref. [30]. To the solution containing 1.24 mg (2.13 μmol) of lapatinib dissolved in 100 μL of DMF 0.8 mg (3.8 μmol) of CN-BFCA and 1.2 μL (8.54 μmol) of triethylamine were added. The mixture was allowed to stay overnight at room temperature under the argon atmosphere and then the solvent was removed under vacuum. The residue was dissolved in a mixture of 100 μL of acetonitrile and the crude product was purified on a semi-preparative HPLC column (system 1), alkalized and lyophilized, yield ≈ 35%.

MS: *m/z*: calc. 675.17; found 676.17 [M + H$^+$], 698.19 [M + Na$^+$].

IR: (KBr plates), cm^{-1}: 2153 (C≡N), 1814, 1785, 1729 (succinimidyl ester).

^{1}H NMR: (CD_3CN) δ (ppm): 2.06 (m, 2H, CH_2–C**H$_2$**–CH_2); 2.90 (t, 2H, CH_2–C**H$_2$**–C(O)–N); 2.93 (s, 3H, C**H$_3$**–S); 3.26 (m, 2H, CH_2–CH_2–N); 3.31 (m, 2H, S–CH_2–CH_2); 3.56 (m, 2H, CN–C**H$_2$**–CH_2); 5.23 (s, 2H, O–C**H$_2$**–C); 6.90 and 7.21 (respectively, d, 1H, C–CH–CH–C and d, 1H, C–CH–C**H**–C, in aromatic ring of furan), 7.15, 7.29, 7.33 and 7.47 (respectively, ddd, 1H, C(F)–C**H**–CH–CH C, d, 1H, C–C**H**–C(F), m, 1H, C(F)–CH–CH–C**H**–C and m, 1H, C(F)–CH–C**H**–CH–C, in aromatic ring of fluorobenzene), 7.20, 7.44 and 7.69 (respectively, d, 1H, C(Cl)–C–C**H**–CH, dd, 1H, C–CH–C**H**–C and d, 1H, C(N)–C**H**–C(Cl) in aromatic ring of chlorobenzene), 8.93, 8.23 and 8.15 (respectively, s, 1H, C–C**H**–C, dd, 1H, C–C**H**–CH and d, 1H, CH–C**H**–C, in aromatic ring of benzene), 8.51 (s, 1H, N–C**H**–N); 8.58 (s, 2H, N–C**H$_2$**–C); 10.88 (s, 1H, C–N**H**–C).

2.3. Synthesis of ^{99m}Tc(NS$_3$)(CN-lapatinib)

The ^{99m}Tc(NS$_3$)(CN-lapatinib) conjugate was synthesized, according to ref. [30] (Scheme 2), in n.c.a. scale in two-steps procedure. In the first step 1 mL of eluate from the ^{99}Mo/^{99m}Tc generator

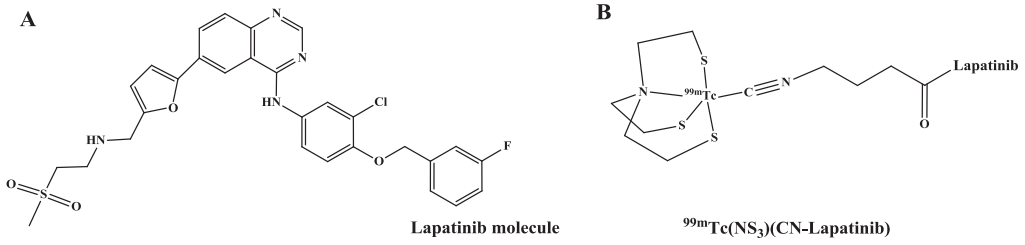

Fig. 1. (A) Lapatinib molecule, (B) ^{99m}Tc labeled lapatinib using the '4+1' approach.

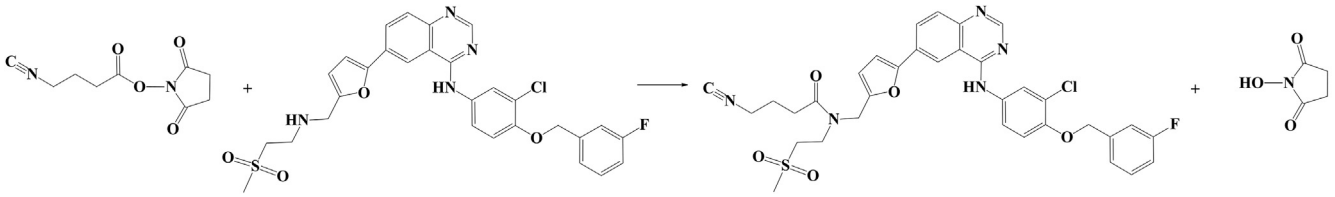

Scheme 1. Coupling reaction of CN-BFCA with lapatinib.

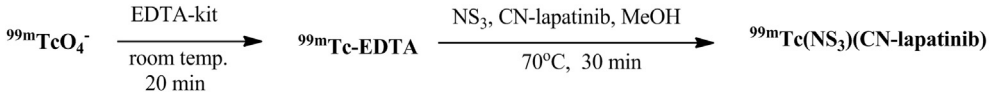

Scheme 2. Two-step synthesis of ^{99m}Tc(NS$_3$)(CN-lapatinib) conjugate in n.c.a. scale.

(200–1000 MBq) was added to a kit formulation containing 1 mg of Na_2EDTA, 5 mg of mannitol and 0.1 mg of $SnCl_2$ in freeze-dried form under nitrogen. The mixture was allowed to stand at room temperature for 20 min. The radiochemical purity was checked by HPLC (System 2) and TLC methods. When Merck 60 WF_{254} aluminum sheets are used the intermediate complex ^{99m}Tc-EDTA/mannitol migrates with the solvent front in water ($R_f = 0.9$) but remains at the origin in acetone ($R_f = 0.1$). In the second step the intermediate ^{99m}Tc-EDTA/mannitol compound reacted with 300 μg of the NS_3 ligand and with about 50 μg of the isocyanide modified with lapatinib molecule. The reaction progress and radiochemical purity were controlled by TLC and HPLC (System 2). The radiochemical yields of the ^{99m}Tc-labeled lapatinib was higher than 97%.

2.4. Synthesis of non-radioactive rhenium reference compound Re(NS$_3$)(CN-lapatinib)

In order to verify the identity of the ^{99m}Tc(NS$_3$)(CN-lapatinib) conjugate synthesized in n.c.a. scale, the non-radioactive rhenium reference conjugate Re(NS$_3$)(CN-lapatinib) was prepared, in milligram scale, in two steps procedure (Scheme 3) starting from the precursor compound Re(NS$_3$)(PMe$_2$Ph), as described previously [31].

In the first step to the stirred solution of 1.0 mg (1.9 μmol) of 'cold rhenium precursor' Re(NS$_3$)(PMe$_2$Ph) dissolved in 500 m μL of $CHCl_3$ 0.51 mg (2.5 μmol) of CN-BFCA was added. The reaction mixture was stirred for 3 h at room temperature under the argon atmosphere. After completion of the reaction (checked by TLC), the solvent was removed under a stream of argon. The main product in this step (Re(NS$_3$)(CN-BFCA)) was purified by column chromatography (SiO_2, THF/Hex, 4:3, v/v). After evaporation of the solvents a green solid was obtained (1.1 mg, yield: 95%).

TOF MS ES$^+$ *m/z*: (Calcd.: [M+H]$^+$: 591.75); Found 591.15 [M+H]$^+$

In the second step to the mixture containing 0.6 mg (1.03 μmol) of lapatinib and 0.71 mg (1.2 μmol) of Re(NS$_3$)(CN-BFCA) dissolved in 100 μL of DMF 0.3 μL (3.72 μmol) of triethylamine was added. The new mixture was stirred for 12 h at room temperature. After completion of the reaction, DMF was removed under vacuum and the residue was dissolved in 200 μL of acetonitrile/water (1:1). The crude product of was purified by HPLC (System 1) and lyophilized. Yield: 40%.

MS for $C_{40}H_{43}N_6O_5ReS_4ClF$, TOF MS ES$^+$ *m/z*: (Calcd.: [M+H]$^+$: 1073.2; Found 1073.7 [M+H]$^+$

^{1}H NMR: (CD_3CN) δ (ppm): 2.08 (m, 2H, CH_2–C**H$_2$**–CH_2); 2.76 (t, 6H, N–C**H$_2$**–CH_2–S), 2.91 (s, 3H, C**H$_3$**–S); 2.92 (t, 2H, CH_2–C**H$_2$**–C(O)–N); 3.09 (m, 6H, N–CH_2–**CH$_2$**–S), 3.23 (m, 2H, CH_2–C**H$_2$**–N); 3.33 (m, 2H, S–C**H$_2$**–CH_2); 3.58 (m, 2H, CN–C**H$_2$**–CH_2); 5.21 (s, 2H, O–C**H$_2$**–C); 6.88 and 7.23 (respectively, d, 1H, C–C**H**–CH–C and d, 1H, C–CH–C**H**–C, in aromatic ring of furan), 7.12, 7.27, 7.31 and 7.46 (respectively, ddd, 1H, C(F)–C**H**–CH–CH C, d, 1H, C–C**H**–C(F), m, 1H, C(F)–CH–CH–C**H**–C and m, 1H, C(F)–CH–C**H**–CH–C, in aromatic ring of fluorobenzene), 7.21, 7.45 and 7.71 (respectively, d, 1H, C(Cl)–C–C**H**–CH, dd, 1H, C–CH–C**H**–C and d, 1H, C(N)–C**H**–C(Cl) in aromatic ring of chlorobenzene), 8.95, 8.24 and 8.17 (respectively, s, 1H, C–C**H**–C, dd, 1H, C–C**H**–CH and d, 1H, CH–C**H**–C, in aromatic ring of benzene), 8.50 (s, 1H, N–C**H**–N); 8.59 (s, 2H, N–C**H$_2$**–C); 10.80 (s, 1H, C–N**H**–C).

2.5. Conditions of HPLC systems

System 1: Phenomenex Jupiter Proteo semipreparative column (4 μm, 90 Å, 250 × 10 mm), UV/Vis detector (220 nm); elution conditions: solvent A – water with 0.1% TFA (v/v); solvent B – acetonitrile with 0.1% TFA (v/v); gradient: 0–20 min 20–80 % of B, 20–35 min 80% solvent B; 2 mL/min;

System 2: Phenomenex Jupiter Proteo analytical column (4 μm, 90 Å, 250 × 4.6 mm), γ-radiation detector; elution conditions: solvent A - water with 0.1% TFA (v/v); solvent B - acetonitrile with 0.1% TFA (v/v); gradient 0–20 min 20–80 % solvent B, 20–35 min 80% solvent B; 1 mL/min.

2.6. TLC

TLC analyses were performed using Merck 60 F_{254} aluminum sheets. All radioactive substances were placed on the strip,

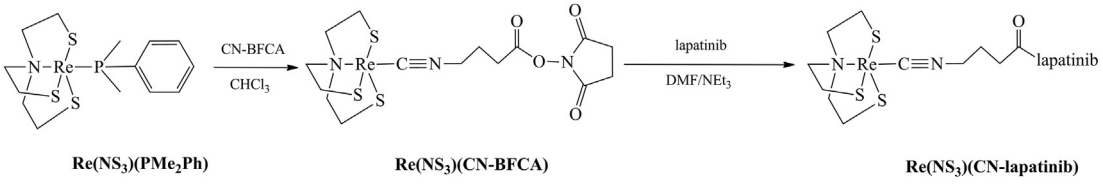

Scheme 3. Synthesis of non-radioactive rhenium reference compound Re(NS$_3$)(CN-lapatinib).

developed with appropriate solutions (water, acetone) and dried. Distribution of radioactivity on the strip was determined using home-made automatic TLC analyzer SC-05 (INCT, Warsaw).

2.7. Challenge experiments

Stability of the isolated ^{99m}Tc(NS$_3$)(CN-lapatinib) conjugate was investigated both as a function of time (HPLC) and in challenge experiments (in the presence of excess of histidine or cysteine), as well as in human serum. The conjugate isolated from the reaction mixture (using HPLC System 1), present in the solution in concentration no higher than 10^{-4} mM, was incubated at 37 °C with 10 mM solutions of histidine or cysteine in the PB buffer (pH 7.4). HPLC analyses of the incubated solutions were performed at different time periods from 0.5 h up to 24 h, since staring the incubation.

2.8. Stability studies

In order to check the stability in human serum 0.1 mL of the solution of the isolated ^{99m}Tc(NS$_3$)(CN-lapatinib) conjugate in the 0.1 M PBS buffer, pH = 7.4, was added to 0.9 mL of human serum (obtained from Sigma Aldrich) and incubated at 37 °C. At specified time intervals small samples (0.1–0.2 mL) of the mixture were withdrawn, mixed in an Eppendorf tube with ethanol (0.3–0.5 mL) and vigorously shaken to precipitate proteins. Then, the samples were centrifuged (14 000 rpm, 5 min) and the supernatant was separated. The radioactivity of both supernatant and precipitate was measured using the well-type NaI(Tl) detector. To check whether the conjugates did not convert into other water-soluble radioactive species, aliquots of the supernatant were analyzed by HPLC for the content of the ^{99m}Tc(NS$_3$)(CN-lapatinib) conjugate.

2.9. Lipophilicity studies

The synthesized conjugate was characterized by determination of the logarithm of its partition coefficient, log P, in the system *n*-octanol/PBS buffer (pH 7.4). The activity of each layer, which shows concentration of the ^{99m}Tc species in the layer, was determined by measuring γ-radiation with a well-type NaI(Tl) detector. Distribution coefficient P was calculated as the ratio of activity of organic to that of aqueous phase (as an average value from at least three independent measurements). Immediately after the distribution experiments, the aqueous phases were analysed by HPLC (System 2) to check whether the studied conjugate had not decomposed during the experiment.

2.10. Biological studies

The biological properties of the conjugate were characterized *in vitro* by investigation of the conjugate affinity to Her-2 receptor using cell line SKOV-3 (human ovarian carcinoma cell line) and *in vivo* by the biodistribution studies. The cells were maintained in ATCC formulated McCOY'S 5A Medium Modified (Catalog No. 30 2007) containing 2 mM of L-Glutamine, 10% of fetal bovine serum supplemented with 0.1 IU/mL penicillin and 0.1 mg/mL streptomycin. Cells were cultured at 37 °C in a humidified incubator under an atmosphere containing 5% of CO_2 and were subcultured once a week. Affinity studies were performed on 6-well plates (SARSTEDT) in McCOY'S 5A Medium which contained approximately 4×10^5 adherent cells in each well. Cell count was determined using hemocytometer and microscope. Preliminary affinity studies were performed by incubating SKOV-3 cells together with the studied conjugate, as well as with other ^{99m}Tc-species, namely with $^{99m}TcO_4^-$, ^{99m}Tc-EDTA-mannitol and ^{99m}Tc(NS$_3$)-mannitol. After 45 min of incubation the binding was stopped, the solution from above the cells was quantitatively separated and the cells were washed three times with cold PBS, pH 7.4 (in order to eliminate unbound radioactivity). Then, the cells were solubilized with 1 M NaOH and activity of solution from above the cells and that of solubilized cells was measured in the gamma counter. Affinity of the conjugate to Her-2 receptor was calculated as the ratio of activity bound by cells to the sum of activity bound by cells and that which remained in the solution above the cells.

In order to determine the K_d value the results of saturation binding experiments (specific bond *vs*. increasing concentration of the conjugate) were analysed by the Scatchard plot using the relationship between the ratio of Specific bound ligand to Free ligand (B/F) *vs*. Specific bound ligand (B). The slope of the straight line shows the negative reciprocal of K_d ($-1/K_d$). The intercept of the straight line with the B axis represents the maximum concentration of conjugate (B_{max}) bound to the Her-2 receptor of cells (represented by the number of binding sites per cell) at infinite conjugate excess.

Competitive binding experiments were performed as follows: 20 000 cpm of ^{99m}Tc(NS$_3$)(CN-lapatinib) in 0.1 M PBS sterile buffer, pH 7.4, was added to each well in 6-well plates in McCOY'S 5A Medium (approximately 5×10^5 cells in each well) and incubated at 37 °C for 45 min. Then, the incubation was stopped and the cells were washed twice with PBS at 37 °C, in order to eliminate unbound activity. Next, the cells were incubated again at 37 °C for 45 min applying concentrations of unlabeled lapatinib in the range 0.016–6250 nM. After that time the incubation was stopped and the solution from above the cells was quantitatively separated and measured in a gamma counter. The cells were again washed twice with PBS at 37 °C, solubilized with 1 M NaOH and counted in a gamma counter. Nonspecific binding was defined as the amount of activity still bound by cells in the presence of 3 μM solution of lapatinib. Under these conditions virtually all receptors are occupied by the unlabeled conjugate, so that the radioconjugate can be bound with cells only *via* nonspecific interactions. The specific binding was obtained by subtracting nonspecific binding from total binding. IC_{50} value was determined from the relationship between the ratio of the activity of the cells to that of quantitatively separated solution from above the cells and concentration of lapatinib. Inhibition constant K_i value was calculated from the IC_{50} value using the Cheng–Prusoff equation [32].

2.11. Biodistribution studies

Biodistribution studies of ^{99m}Tc(NS$_3$)(CN-lapatinib) conjugate (Table 1) were performed on normal 3 months old male BALB/c mice (of weight between 23 and 28 g, $n = 12$), according to the relevant national regulations. The mice were injected *via* tail vein with 3.02–3.66 MBq in 200–210 μL of aqueous solution of ^{99m}Tc(NS$_3$)(CN-lapatinib) and sacrificed at 30 min and 60 min after injection of conjugate. Then, tissues were dissected, washed free of

Table 1
Biodistribution studies of ^{99m}Tc(NS$_3$)(CN-lapatinib) conjugate in BALB/c mice at 30 and 60 min post injection ($n = 6$, % ID/g ± S.D.).

Organ	30 min	60 min
Heart	0.10 ± 0.02	0.92 ± 0.04
Kidneys	3.28 ± 0.4	4.98 ± 0.6
Liver	4.89 ± 0.9	4.55 ± 0.8
Lungs	0.77 ± 0.08	0.56 ± 0.09
Spleen	0.44 ± 0.3	0.38 ± 0.02
Blood	0.99 ± 0.01	0.48 ± 0.02
Thyroid	0.94 ± 0.04	0.38 ± 0.02

blood and weighed. Associated radioactivity was counted using gamma counter. The accumulated radioactivity in the tissue of organs was calculated as the percentage of injected dose per gram (% ID/g) of tissue, as well as the percentage of injected dose per gram of blood. The standard source of ^{99m}Tc was also measured simultaneously with the samples in order to perform the decay correction.

3. Results and discussion

3.1. Lapatinib labeling, stability and lipophilicity studies

The conjugate ^{99m}Tc(NS$_3$)(CN-lapatinib) is formed with high yield > 97%, high purity > 98%, (Fig. 2) and with specific activity within the range 25–30 GBq/μmol. The small peaks recorded at R_T = 3.4 min and 7.9 min correspond to the intermediate complexes ^{99m}Tc-EDTA-mannitol and ^{99m}Tc(NS$_3$)-mannitol, respectively. In the ^{99m}Tc(NS$_3$)(CN-lapatinib) conjugate the NS$_3$ ligand coordinates the ^{99m}Tc(III) cation and leaves the fifth coordination site free and available for one monodentate isocyanide ligand previously coupled with the lapatinib molecule.

The HPLC chromatograms of ^{99m}Tc(NS$_3$)(CN-lapatinib) and Re(NS$_3$)(CN-lapatinib) conjugates, obtained exactly under the same conditions, are shown in Fig. 2. As one can see the peak positions of both conjugates are very close (R_T values are 18.4 min and 18.5 min for Re(NS$_3$)(CN-lapatinib) and ^{99m}Tc(NS$_3$)(CN-lapatinib), respectively). Almost the same R_T values of both species can be a proof of the existence of the ^{99m}Tc(NS$_3$)(CN-lapatinib) compound in the reaction mixture in n.c.a. scale.

Stability of the ^{99m}Tc(NS$_3$)(CN-lapatinib) conjugate was studied in “challenge experiments”, in the presence of 1000 times the molar excess of histidine and cysteine. In both cases the HPLC chromatograms, recorded after 24 h of incubation, showed presence of only one radioactive species in the solution, with the retention time characteristic for the studied conjugate. Thus, we can consider that the conjugate does not undergo the ligand exchange reaction with amino acids or other strongly competing natural ligands containing SH or NH groups.

Stability studies of the ^{99m}Tc(NS$_3$)(CN-lapatinib) conjugate in human serum confirmed that the conjugate, containing the non-peptidic synthetic compound lapatinib, does not undergo the enzymatic biodegradation. The HPLC chromatogram recorded after 24 h showed only one peak with the retention time corresponding to that of ^{99m}Tc(NS$_3$)(CN-lapatinib) compound. The measurements of radioactivity of both the supernatant and precipitate (protein) fractions indicated that the percentage of ^{99m}Tc(NS$_3$)(CN-lapatinib) conjugate, which has been bound by the serum components, was in the range of 8–10%.

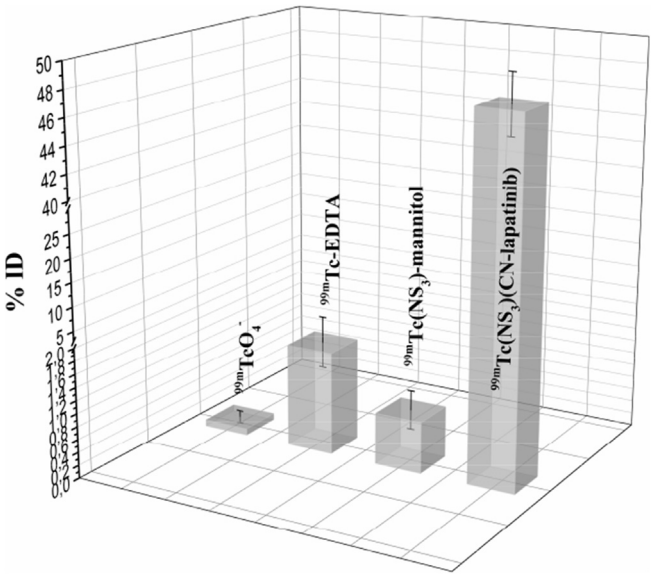

Fig. 3. Cell binding of ^{99m}Tc(NS$_3$)(CN-lapatinib) conjugate in comparison with other ^{99m}Tc-species. Cell binding levels are expressed as the percentage of added doses (%ID).

The determined lipophilicity value of the ^{99m}Tc(NS$_3$)(CN-lapatinib) conjugate was found to be 1.24 ± 0.04 (n = 4). Contrary to trastuzumab (humanized IgG1 monoclonal antibody of molecular mass equal to 145531.5 g/mol) labeled with diagnostic radionuclides, the ^{99m}Tc(NS$_3$)(CN-lapatinib) conjugate of molecular mass equal to 968.5 g/mol is characterized by significantly lower molecular weight and lipophilicity appropriate for distribution in the body. Both these properties make the conjugate distribution easier and more efficient. According to literature data the value of molecular mass of the compound, suitable for the blood-tissue barrier crossing, should be approximately lower than 500 Da and the lipophilicity value should be within the range 1–4 [33]. The lipophilicity of the ^{99m}Tc(NS$_3$)(CN-lapatinib) conjugate can be easily modified by introduction of a hydrophilic or hydrophobic group at the periphery of the NS$_3$ ligand does not affect the synthesis reaction of the conjugate and its stability [34].

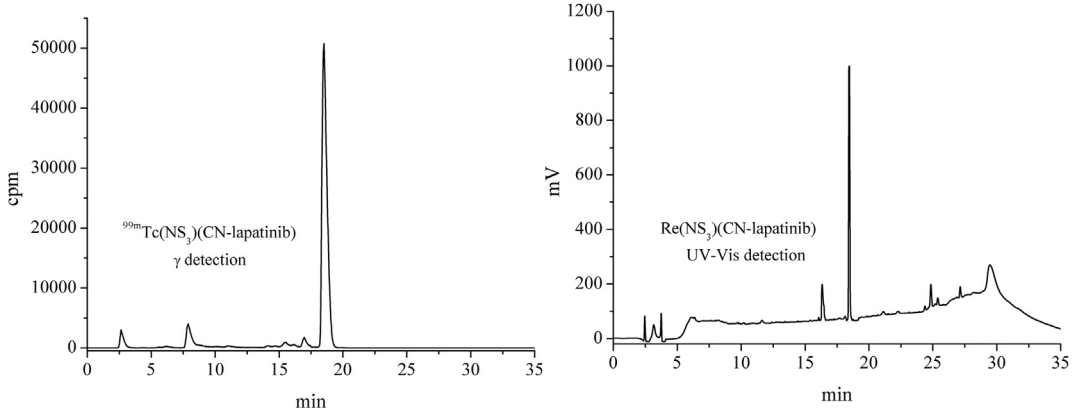

Fig. 2. The HPLC chromatograms of the Tc- and Re-labeled lapatinib conjugates prepared in this study (performed in system 2).

3.2. Binding studies

The pilot affinity studies performed with the ^{99m}Tc(NS$_3$)(CN-lapatinib) conjugate as well as with other ^{99m}Tc-species ($^{99m}TcO_4^-$, intermediate compounds ^{99m}Tc-EDTA-mannitol and ^{99m}Tc(NS$_3$)-mannitol) are shown in Fig. 3. As one can see only ^{99m}Tc(NS$_3$)(CN-lapatinib) conjugate, containing lapatinib molecule, interacts with Her-2 receptors.

Saturation binding experiments (performed in the system specific bond *vs*. increasing concentration of the conjugate) have shown that binding of the ^{99m}Tc(NS$_3$)(CN-lapatinib) conjugate to Her-2 receptor of SKOV-3 cells is saturable and specific in the predominant degree (Fig. 4(A)). The non-specific binding determined in the presence of 0.1 μM solution of lapatinib accounts in general for about 0.3% of specific binding. The B_{max} value was found to be 2.4 ± 0.3 nM ($n = 3$) which corresponds to the approximate number of 2.4×10^6 binding sites per cell (Fig. 4(A)). The dissociation constant K_d, determined from the Scatchard plot (Fig. 4(B)), was found to be 3.5 ± 0.4 nM ($n = 3$).

In the competitive binding experiment the unlabeled lapatinib molecules inhibited binding of the ^{99m}Tc(NS$_3$)(CN-lapatinib) conjugate to Her-2 receptor. The inhibitory concentration of 50% (IC_{50}) obtained for lapatinib was found to be 41.2 ± 0.4 nM (Fig. 5). Inhibition constant K_i value, calculated from the IC_{50} value using the Cheng–Prusoff equation, was found to be 2.9 ± 0.5 nM.

Comparison of the results obtained for ^{99m}Tc(NS$_3$)(CN-lapatinib) conjugate with those obtained for trastuzumab labeled with diagnostic radionuclides shows that ^{99m}Tc-labeled lapatinib is equipped with better biological properties. However, in such comparison it is necessary to keep in mind that the experimentally determined values characterizing biological behavior of the studied species depend strongly upon the experimental conditions. This is because binding reaction is temperature dependent and tissue is temperature sensitive. Moreover, the same type of receptor expressed on cell surface of different cell lines can exhibit different biological behavior. Therefore, the experimentally obtained values, measured under different experimental conditions and in different laboratories, can not be considered as 'absolute' and their comparison can be only qualitative.

The K_d value of ^{99m}Tc(NS$_3$)(CN-lapatinib) conjugate (equal to 3.5 nM) is comparable with that of trastuzumab labeled with At-211 (K_d value of ^{211}At-trastuzumab, calculated from k_{on} and k_{off} values presented in the paper [26], is equal to 1.46 nM. The low K_d value of ^{99m}Tc(NS$_3$)(CN-lapatinib) conjugate indicates its high affinity to Her-2 receptors on the SKOV-3 line cells. The number of available binding sites on a single SKOV-3 cell was found to be

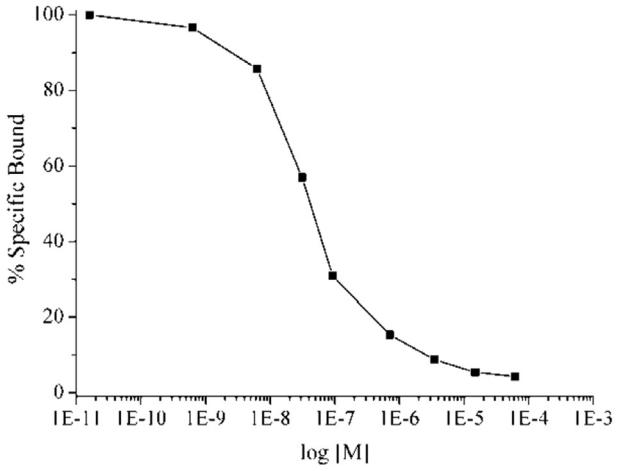

Fig. 5. Displacement of ^{99m}Tc(NS$_3$)(CN-lapatinib) by increasing concentration of unlabeled lapatinib.

2.4×10^6. This value is about twice higher, in comparison with those of trastuzumab labeled with e.g. lutetium-177 (1×10^6) [25] or with astatine-211 (1.5×10^6) [26].

3.3. Biodistribution studies

Biodistribution studies of ^{99m}Tc(NS$_3$)(CN-lapatinib) conjugate in BALB/c mice showed generally low conjugate uptake (<5 %ID/g) in all studied organs, slightly higher uptake in liver (4–5 %ID/g) than in kidney (3–5 %ID/g) (Table 1). This points out to the clearance of the ^{99m}Tc(NS$_3$)(CN-lapatinib) conjugate through the hepatic and renal route in comparable degree. The uptake in other organs remained on the level <1 %ID/g.

Basing on physicochemical and biological studies of ^{99m}Tc(NS$_3$)(CN-lapatinib) conjugate one can see the superiority of the studied conjugate, in comparison with trastuzumab labeled with diagnostic radionuclides. Moreover, contrary to trastuzumab, lapatinib does not affect the heart (in women treated with trastuzumab a cardiac dysfunction is usually observed [35]). It is also worth noting the significantly lower costs of lapatinib-based radiopharmaceuticals, as compared with those based on labeled trastuzumab. Taking into account easy availability of technetium-99m radionuclide (from the portable ^{99}Mo-^{99m}Tc generator), in comparison with availability of positron-emitting radionuclides C-11 and F-18, as well as the synthesis routes of potential lapatinib-based radiopharmaceuticals containing these radionuclides, the

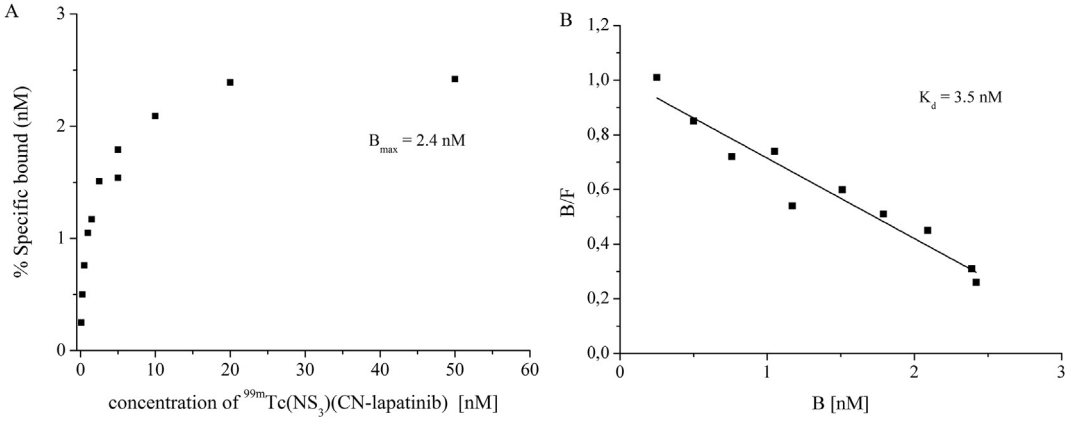

Fig. 4. (A) The saturation curve for ^{99m}Tc(NS$_3$)(CN-lapatinib). The specifically bound radioligand is plotted as a function of increasing concentrations of ^{99m}Tc(NS$_3$)(CN-lapatinib). (B) Scatchard plot.

^{99m}Tc(NS$_3$)(CN-lapatinib) conjugate seems to be an imaging agent superior to [^{11}C]Lapatinib [36] and [^{18}F]Lapatinib [37] compounds.

4. Conclusions

^{99m}Tc(NS$_3$)(CN-lapatinib) conjugate is formed with high yield and presents high stability in solutions containing competitive cysteine/histidine ligands. The biological *in vitro* and *in vivo* studies of the conjugate showed its high affinity to Her-2 receptor and the clearance through the hepatic and renal route in comparable degree. From the point of view of application in nuclear medicine it is important to note that the ^{99m}Tc(NS$_3$)(CN-lapatinib) conjugate can be easily synthesized in hospital laboratories from the previously prepared lyophilized kit formulations.

Concluding, the ^{99m}Tc(NS$_3$)(CN-lapatinib) conjugate may be considered to be a promising diagnostic radiopharmaceutical for patients suffering from breast cancer of Her-2 type and to be a useful tool for stratification of patients for the so-called personalised therapy.

Acknowledgments

The work was carried out within the grant No: N R13 0150 10 (National Centre for Research and Development – NCBiR). The authors thank Prof. S. Siekierski (INCT, Warsaw, Poland) for valuable discussions and review of the manuscript.

References

[1] C.F. Matthew, D.C. Kendall, F.V. Felix, J.L. Daniel, M. De vos Abraham, X.S. Mark, Insights into ErbB signaling from the structure of the ErbB2-pertuzumab complex, Cancer Cell. 5 (2004) 317–328.
[2] P. Morrow, F. Zambrana, F.J. Esteva, Recent advances in systemic therapy: advances in systemic therapy for HER2-positive metastatic breast cancer, Breast Cancer Res. 11 (2009) 207–217.
[3] J.S. Ross, J.A. Fletcher, G.P. Linette, J. Stec, E. Clark, M. Ayers, W.F. Symmans, L. Pusztai, K.J. Bloom, The Her-2/neu gene and protein in breast cancer: biomarker and target of therapy, Oncologist 8 (2003) 307–325.
[4] E. Verri, P. Guglielmini, M. Puntoni, L. Perdelli, A. Papadia, P. Lorenzi, A. Rubagotti, N. Ragni, F. Boccardo, HER2/neu oncoprotein overexpression in epithelial ovarian cancer: evaluation of its prevalence and prognostic significance. Clinical Study, Oncology 68 (2005) 154–161.
[5] E.V. Høgdall, L. Christensen, S.K. Kjaer, J. Blaakaer, J.E. Bock, E. Glud, B. Nørgaard-Pedersen, C.K. Høgdall, Distribution of HER-2 overexpression in ovarian carcinoma tissue and its prognostic value in patients with ovarian carcinoma: from the Danish MALOVA Ovarian Cancer Study, Cancer 98 (2003) 66–73.
[6] S.B. Kolla, A. Seth, M.K. Singh, N.P. Gupta, A.K. Hemal, P.N. Dogra, L. Kumar, Prognostic significance of Her2/neu overexpression in patients with muscle invasive urinary bladder cancer treated with radical cystectomy, Int. Urol. Nephrol. 40 (2008) 321–327.
[7] H. Nakamura, N. Kawasaki, M. Taguchi, K. Kabasawa, Association of HER-2 overexpression with prognosis in nonsmall cell lung carcinoma: a meta-analysis, Cancer 103 (2005) 1865–1873.
[8] M. Salem, Y. Kinoshita, T. Tajiri, R. Souzaki, K. Tatsuta, M. Higashi, T. Izaki, K. Kohashi, M. Tsuneyoshi, T. Taguchi, Association between the Her-2 expression and histological differentiation in Wilms tumor, Pediatr. Surg. Int. 22 (2006) 891–896.
[9] H. Fiegl, S. Millinger, G. Goebel, E. Holzner, C. Marth, P.W. Laird, M. Widschwendter, Breast cancer DNA methylation profiles in cancer cells and tumor stroma: aassociation with HER-2/neu status in primary breast cancer, Cancer Res. 66 (2006) 29–33.
[10] S. Ménard, S.M. Pupa, M. Campiglio, E. Tagliabue, Biologic and therapeutic role of HER2 in cancer, Oncogene 22 (2003) 6570–6578.
[11] T. Kute, C.M. Lack, M. Willingham, B. Bishwokama, H. Williams, K. Barrett, T. Mitchell, J.P. Vaughn, Development of herceptin resistance in breast cancer cells, Cytometry 57A (2004) 86–93.
[12] H.A. Burris III, Dual kinase inhibition in the treatment of breast cancer: initial experience with the EGFR/ErbB-2 inhibitor lapatinib, Oncologist 9 (2004) 10–15.
[13] C.M. Ellis, M.J. Dyson, T.J. Stephenson, E.L. Maltby, HER2 amplification status in breast cancer: a comparison between immunohistochemical staining and fluorescence in situ hybridisation using manual and automated quantitative image analysis scoring techniques, J. Clin. Pathol. 58 (2005) 710–714.
[14] G. Sauter, J. Lee, J.M. Bartlett, D.J. Slamon, M.F. Press, Guidelines for human epidermal growth factor receptor 2 testing: biologic and methodologic considerations, J. Clin. Oncol. 27 (2009) 1323–1333.
[15] M. Pedersen, B.B. Rasmussen, The correlation between dual-color chromogenic in situ hybridization and fluorescence in situ hybridization in assessing HER2 gene amplification in breast cancer, Diagn. Mol. Pathol. 18 (2009) 96–102.
[16] M. Tanner, D. Gancberg, A. Di Leo, D. Larsimont, G. Rouas, M.J. Piccart, J. Isola, Chromogenic in situ hybridization: a practical alternative for fluorescence in situ hybridization to detect HeR-2/neu oncogene amplification in archival breast cancer samples, Am. J. Pathol. 157 (2000) 1467–1472.
[17] V. Calzada, F. Garcia, M. Fernández, W. Porcal, T. Quinn, O. Alonso, J.P. Gambini, P. Cabral, Labeling and biological evaluation of Tc-HYNIC-trastuzumab as a potential radiopharmaceutical for *in vivo* evaluation of HER2 expression in breast Cancer, World J. Nucl. Med. 12 (2013) 27–32.
[18] M.N. Lub-de Hooge, J.G.W. Kosterink, P.J. Perik, H. Nijnuis, L. Tran, J. Bart, J.H.A. Suurmeijer, S. de Jong, L.P. Jager, G.E.E. de Vries, Preclinical characterisation of ^{111}In-DTPA-trastuzumab, Br. J. Pharm. 143 (2004) 99–106.
[19] E.C.F. Dijkers, J.G.W. Kosterink, A.P. Rademaker, L.R. Perk, A.M.S.G. Van Dongen, J. Bart, R.J. de Jong, G.E.E. de Vries, N.M. Lub-de Hooge, Development and characterization of clinical-grade ^{89}Zr-Trastuzumab for HER2/neu Immuno-PET imaging, J. Nucl. Med. 50 (2009) 974–981.
[20] E.C. Dijkers, T.H.O. Munnink, J.G.W. Kosterink, A.H. Brouwers, P.L. Jager, J.R. de Jong, G.A. van Dongen, C.P. Schröder, M.N. Lub-de Hooge, E.G. de Vries, Biodistribution of ^{89}Zr-trastuzumab and PET imaging of HER2-positive Lesions in patients with metastatic breast Cancer, Clin. Pharmacol. Ther. 87 (2010) 586–592.
[21] B. Alirezapoura, A.R. Jalilianb, F. Bolourinovin, S. Moradkhani, Production and quality control of [^{67}Ga]-DOTA-trastuzumab for radioimmunoscintigraphy, Iran. J. Pharm. Res. 12 (2013) 355–366.
[22] K. Tamura, H. Kurihara, K. Yonemori, H. Tsuda, J. Suzuki, Y. Kono, N. Honda, M. Kodaira, H. Yamamoto, M. Yunokawa, C. Shimizu, K. Hasegawa, Y. Kanayama, S. Nozaki, T. Kinoshita, Y. Wada, S. Tazawa, K. Takahashi, Y. Watanabe, Y. Fujiwara, ^{64}Cu-DOTA-trastuzumab PET imaging in patients with HER2-positive breast cancer, J. Nucl. Med. 54 (2013) 1869–1875.
[23] M. Pruszynski, E. Koumarianou, G. Vaidyanathan, H. Revets, N. Devoogdt, T. Lahoutte, M.R. Zalutsky, Targeting breast carcinoma with radioiodinated anti-HER2 nanobody, Nucl. Med. Biol. 40 (2013) 52–59.
[24] M. Pruszynski, E. Koumarianou, G. Vaidyanathan, H. Revets, N. Devoogdt, T. Lahoutte, H.K. Lyerly, M.R. Zalutsky, Improved tumor targeting of anti-HER2 nanobody through n-succinimidyl 4-guanidinomethyl-3-iodobenzoate radiolabeling, J. Nucl. Med. 55 (2014) 650–656.
[25] G.L. Ray, K.E. Baidoo, L.M.M. Keller, P.S. Albert, M.W. Brechbiel, D.E. Milenic, Pre-clinical assessment of ^{177}Lu-Labeled trastuzumab targeting HER2 for treatment and management of cancer patients with disseminated intraperitoneal disease, Pharmaceuticals 5 (2012) 1–15.
[26] S. Palm, T. Bäck, L. Claesson, A. Danielsson, J. Elgqvist, S. Frost, R. Hultborn, H. Jensen, S. Lindegren, L. Jacobsson, Therapeutic efficacy of astatine-211–labeled trastuzumab on radioresistant SKOV-3 tumors in nude mice, Int. J. Radiat. Oncol. Biol. Phys. 69 (2007) 572–579.
[27] C.S. Cutler, H.M. Hennkens, N. Sisay, S. Huclier-Markai, S.S. Jurisson, Radiometals for combined imaging and therapy, Chem. Rev. 113 (2013) 858–883.
[28] H. Spies, M. Glaser, H.-J. Pietzsch, F.E. Hahn, T. Luegger, Synthesis and reactions of trigonal-bipyramidal rhenium and technetium complexes with a tripodal, tetradentate NS$_3$ ligand, Inorg. Chim. Acta 240 (1995) 465–478.
[29] J.-U. Kuenstler, B. Veerenda, S.D. Figueroa, G.L. Sieckman, T.L. Rold, T.J. Hoffman, C.J. Smith, H.-J. Pietzsch, Organometallic ^{99m}Tc(III) '4+1' Bombesin(7-14) conjugates: synthesis, radiolabeling, and *in Vitro/in vivo* studies, Bioconjugate Chem. 18 (2007) 1651–1661.
[30] S. Seifert, J.-U. Kuenstler, E. Schiller, H.-J. Pietzsch, B. Pawelke, R. Bergmann, H. Spies, Novel procedures for preparing ^{99m}Tc(III) complexes with tetradentate/monodentate coordination of varying lipophilicity and adaptation to ^{188}Re analogues, Bioconjugate Chem. 15 (2004) 856–863.
[31] E. Schiller, S. Seifert, F. Tisato, F. Refosco, W. Kraus, H. Spies, H.-J. Pietzsch, Mixed-ligand Rhenium-188 complexes with Tetradentate/Monodentate NS$_3$/P ('4+1') coordination: relation of structure with antioxidation stability, Bioconjugate Chem. 16 (2005) 634–643.
[32] Y. Cheng, W. Prusoff, Relationship between the inhibition constant (K_i) and the concentration of inhibitor which causes 50 per cent inhibition (IC_{50}) of an enzymatic reaction, Biochem. Pharmacol. 33 (1973) 3099–3108.
[33] V. Pike, PET Radiotracers: crossing the blood-brain barrier and surviving metabolism, Trends Pharmacol. Sci. 30 (2009) 431–440.
[34] J.-U. Kunstler, G. Seidel, R. Bergmann, E. Gniazdowska, M. Walther, E. Schiller, C. Decristoforo, H. Stephan, R. Roland Haubner, J. Steinbach, H.-J. Pietzsch, Novel ^{99m}Tc '4+1' peptide conjugates: tuning the biodistribution by variation of coligands, Eur. J. Med. Chem. 45 (2010) 3645–3655.
[35] A. Seidman, C. Hudis, M.K. Pierri, S. Shak, V. Paton, M. Ashby, M. Murphy, S.J. Stewart, D. Keefe, Cardiac dysfunction in the trastuzumab clinical trials experience, J. Clin. Oncol. 20 (2002) 1215–1221.
[36] M. Huiban, S. Hill, R. Reiley, G. Singleton, T. Kihlberg, R. Owenius, A. Gunnar, J. Passchier, [^{11}C]Lapatinib for PET imaging of brain metastasis in human subjects with breast cancer, J. Label. Compd. Radiopharm. 54 (2011) S194.
[37] F. Basuli, H. Wu, Ch Li, Z.-D. Shi, A. Sulima, G.L. Griffiths, A first synthesis of [^{18}F]Lapatinib: a potential tracer for positron emission tomographic imaging of ErbB1/ErbB2 tyrosine kinase activity, J. Label. Compd. Radiopharm. 54 (2011) S474.